

Evidence for Arcing on the International Space Station Solar Arrays

Joseph I. Minow, Ira Katz, Paul D. Craven, Victoria A. Davis, Barbara M. Gardner, Thomas W. Kerslake, Myron J. Mandell, Linda Neergaard Parker, Timothy J. Peshek, Emily M. Willis, and Kenneth H. Wright, Jr.

Abstract—The International Space Station (ISS) is powered by a set of 160 V photovoltaic arrays (PVA) in the US sector. Arcing thresholds for the ISS PVAs measured in the laboratory are shown to vary from -210 V to -457 V depending on the ambient plasma density, where low arcing threshold occurs at high plasma densities. Arcing of ISS PVAs on-orbit is unlikely under normal operating conditions. The net potential of a solar cell relative to space depends on the position of the cell within a string, the $(v \times B) \cdot L$ contribution to the potential at the location of the cell, and the frame potential of ISS due to solar array charging. Net potentials on a cell will reach the arcing threshold only on rare occasions. However, the situation changes when damaged PVA strings are considered. Open circuit strings can exhibit voltages exceeding -300 V when the strings are shunted. Under these conditions the local potential on the damaged string can easily exceed arcing thresholds at the low end of the -210 V to -457 V range for ISS PVAs. Because arcing to space on the array will remove some fraction of the net negative charge on the ISS, transient variations in the frame potential are expected during the electrostatic discharge events. We report a new class of transient ISS frame potential variations consistent with arcing on open strings using data from the ISS Floating Potential Measurement Unit's Floating Potential Probe instrument.

Index Terms— arcing, spacecraft charging, solar arrays

I. INTRODUCTION

THE International Space Station (ISS) is powered by a set of 160 V photovoltaic arrays (PVA) in the US sector with the negative end of the arrays grounded to the conducting

structure of the ISS. This configuration represents a possible risk to arcing if the voltage on any local portion of the arrays or vehicle structure exceeds the arcing threshold for the materials at that location. The rule of thumb often used for high voltage solar arrays is that the most negative surfaces will float to a negative potential that is about 90% of the solar array operating voltage [1, 2]. An example of a spacecraft that followed this rule was the Upper Atmospheric Research Satellite (UARS) with 100 V solar arrays grounded on the negative end of the array to the spacecraft structure. The structure was regularly seen to charge to -90 V relative to the space plasma environments at eclipse exit due to plasma interactions with the solar arrays [3].

While negative potentials on the ISS structure are regularly observed each orbit as the vehicle enters insolation, potentials on the ISS structure only rarely approach the less than -70 V thresholds where arcing could be observed [4,5]. Arcing thresholds for the ISS PVAs measured in the laboratory are shown to vary from -210 V to -457 V depending on the ambient plasma density, where low arcing threshold occurs at high plasma densities [6]. Arcing of ISS PVAs on-orbit is unlikely under normal operating conditions. The net potential of a solar cell relative to space depends on the position of the cell within the 160 V string, the $v \times B \cdot L$ contribution to the potential at the location of the cell, and the frame potential of ISS due to solar array charging. Net potentials on a cell will barely reach the arcing threshold only on rare occasions. Up to the current time, arcing has not been reported on either the ISS structure or the solar arrays.

In this paper we report a new class of transient ISS frame potential variations consistent with arcing using data from the ISS Floating Potential Measurement Unit's (FPMU) Floating Potential Probe (FPP) instrument. The transients are characterized by a rapid decrease in the negative frame potential

J.I. Minow is the NASA Technical Fellow for Space Environments and is located at Marshall Space Flight Center, Huntsville, AL 35812 USA (e-mail: joseph.minow@nasa.gov).

I. Katz is with The Jet Propulsion Laboratory, Pasadena, CA 91109 (e-mail: ira.katz@jpl.nasa.edu).

P.D. Craven is with NASA Marshall Space Flight Center, Huntsville, AL 35812 (e-mail: paul.craven@nasa.gov).

V.A. Davis is with Leidos, San Diego, CA 92121 (e-mail: Victoria.A.Davis@leidos.com).

B.M. Gardner is with Leidos, Leidos, San Diego, CA 92121 (e-mail: barbara.m.gardner@leidos.com).

T.W. Kerslake is with NASA Glenn Research Center, Cleveland, OH 44135 (e-mail: thomas.w.kerslake@nasa.gov).

M.J. Mandell is with Leidos, San Diego, CA 92121 (e-mail: myron.j.mandell@leidos.com).

T.J. Peshek is with NASA Glenn Research Center, Cleveland, OH 44135 (e-mail: timothy.j.peshek@nasa.gov).

L.N. Parker is with Universities Space Research Association, Huntsville, AL 35805 (e-mail: lparker@usra.edu).

E.M. Willis is with NASA Marshall Space Flight Center, Huntsville, AL 35812 (e-mail: emily.willis@nasa.gov).

K.H. Wright, Jr. is with Universities Space Research Association, Huntsville, AL 35805 (e-mail: kwright@usra.edu).

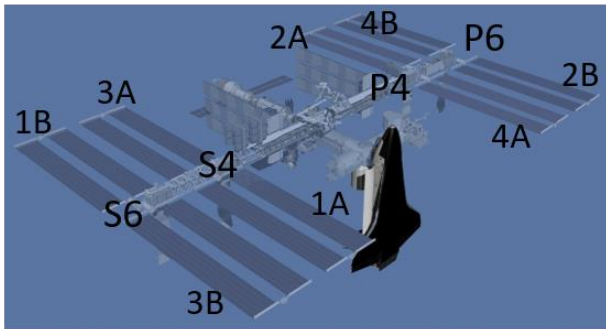


Fig. 1. ISS high voltage solar array configuration (NASA image)

to values less negative, or even positive, than the equilibrium potential followed by a gradual return to equilibrium conditions. The events are always observed in sunlight when the PVAs are biased and occur during periods when some or all of the PVA strings are shunted.

The outline of this paper is as follows. First, Section II provides a background on the ISS orbital environment and the configuration of the ISS PVAs. The FPMU instrument that provides the ISS frame potential data used in this work is described next in Section III. Section IV summarizes the ISS negative charging due to current collection by the high-voltage solar arrays. An explanation of how open-circuit voltages present on damaged strings can exceed arcing thresholds on the solar arrays is given in Section V. The new class of “positive charging” events consistent with arcing on the arrays are described in Section VI. Finally, we conclude with a short discussion and summary in Section VII.

II. ISS ORBITAL ENVIRONMENT AND CONFIGURATION OF PVAS

Inclination of the ISS orbit is 51.6 degrees with an orbital altitude varying between about 330 km and 435 km. Flight altitudes in recent years have typically been near 400 km. This places ISS operations within the F2-region of the Earth’s ionosphere, at an altitude near the peak F2-region electron density or in the topside ionosphere. Ion and electron temperatures in this region of the ionosphere are on the order of 0.1 eV [7] so the voltages on conductors exposed to the plasma environment including the solar cells and components of the vehicle structure connected to the spacecraft ground will control the current collection process responsible for establishing the frame potential relative to the space plasma environment.

The 160 V ISS solar arrays are configured into eight solar array wings (SAW) with two blankets per wing and two solar array wings per Photovoltaic Module (PVM) and a total of four PVM on ISS [8]. Fig. 1 shows the layout of the eight arrays with the nomenclature used by the ISS program for labeling the eight SAWs (1A, 1B, 2A, 2B, 3A, 3B, 4A, and 4B) and the four PVM’s (S4 and S6 on the starboard Truss and P4 and P6 on the port Truss). Each of the eight 11.7 m wide by 35.1 m long arrays are covered with 8 cm x 8 cm silicon solar cells laid out in 82 parallel strings with 400 cells in series per string. There

are 32,800 solar cells per SAW for a total of 262,400 total cells in the eight ISS SAWs. The negative end of the eight US solar arrays are all electrically tied to a common point ground on the metal ISS structure [8,9,10].

The SAWs are connected to Sequential Shunt Units (SSU) which maintain the PVA voltage at 160 V and regulates the ISS power production from PVAs to meet ISS power load demand [8]. Solid-state switches in the SSU operating at 20 Hz will dynamically shunt power from the 82 individual strings to follow load demand as required to charge the ISS storage batteries [8,9]. The shunt operations to reduce power output from the array is accomplished by short-circuiting an individual string so there is no voltage across the string [10]. Since power output of the string P is given by $P=IV$ where I is the operating current and V the operating voltage for the string of cells in series, the shunt sets the string voltage to $V=0$ and there is no power output for the string. Each of the 82 strings are connected or disconnected from the primary bus and the power output from the SSU is the sum of all connected strings at any point in time. When power output from the SSU exceeds the ISS power demand, the SSU will shunt PVA strings to reduce the power output. If SSU power output is insufficient for ISS power demand, the SSU will unshunt the strings required to provide the additional power to meet demand.

Spacecraft charging of the ISS is driven primarily by current collection at the edges of the solar cells on the 160 V solar arrays in the US sector. The potential of each cell varies from 0 V to 160 V along the string but the solar array string voltage relative to the local plasma environment will come to an equilibrium such that electron collection by the solar array balances ion collection by various grounded, conductive surfaces. The vehicle structure, since it is grounded on the negative end of the arrays, will collect ions and float negative relative to the plasma [11, 12, 13, 14].

ISS is equipped with two operational Plasma Contactor Units (PCU) used for active charge control to mitigate the effects of extreme charging [15, 16]. The PCU’s are hollow cathode discharge assemblies which produces a cloud of ionized xenon gas that carries excess electron charge away from the ISS



Fig. 2. The Floating Potential Measurement Unit (FPMU) showing the location of the WLP, NLP, FPP, and PIP as well as the electronics box and TVCIC (NASA image).

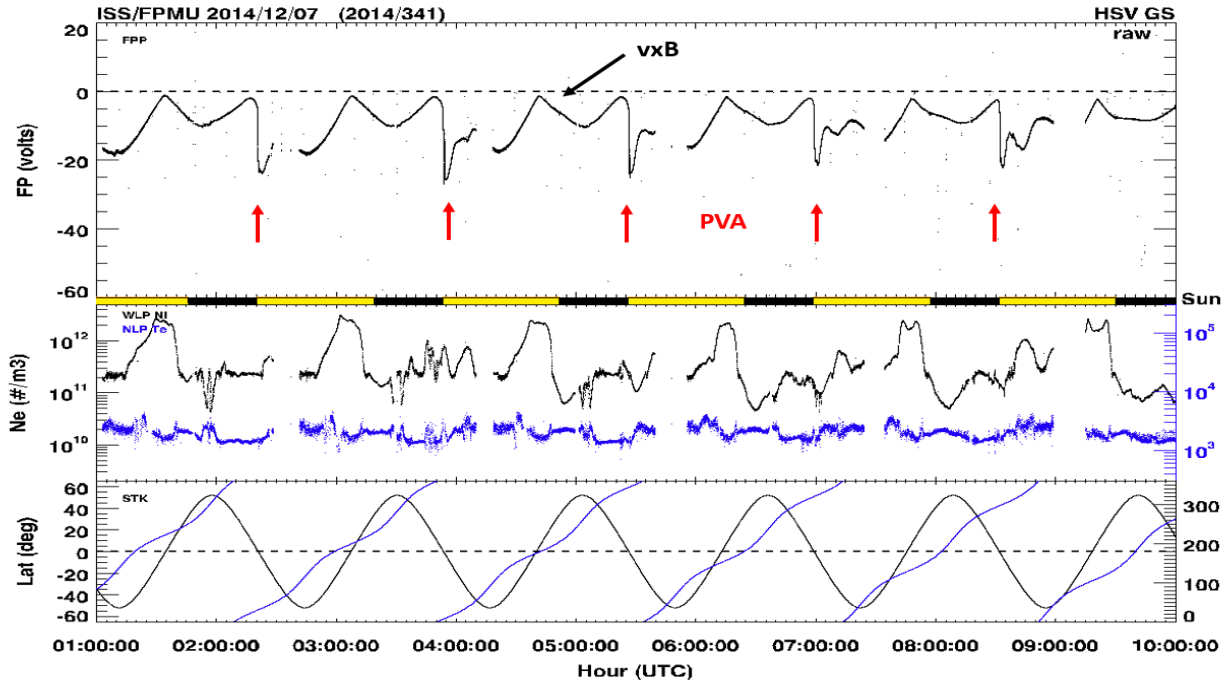


Fig. 3. Example FPMU data for six orbits on 7 December 2014. ISS floating potential obtained from the FPP is plotted in the top panel. The middle panel gives the WLP electron density (black) and NLP electron temperature (blue). Geographic latitude (black) and longitude (blue) are shown in the bottom panel. Details are discussed in the text.

structure into the surround space plasma, reducing the potential difference between the Station structure and the surrounding charged plasma environment. We have only chosen FPMU records for this work where the PCUs are not operating.

III. FLOATING POTENTIAL MEASUREMENT UNIT

The Floating Potential Measurement Unit (Fig. 2) is a suite of four plasma instruments deployed on the ISS in August of 2006. It was designed and built by Space Dynamics Laboratory located in Logan, Utah under contract to NASA Johnson Space Center. While the reported FPMU design life of the was only three years, the current operational unit on ISS was deployed in August of 2006 and has continued to provide data to the present time, a period exceeding 11 years! Details on the instrument design and operations are given in a series of references including [17], [18], [19], [20], and [21].

FPMU is a suite of four instruments including a Wide Langmuir Probe (WLP), a Narrow Langmuir Probe (NLP), a Floating Potential Probe (FPP), and a Plasma Impedance probe (PIP). The WLP and NLP provide measurements of electron density, electron temperature, and frame potential relative to the ambient space plasma at a sample rate of 1.0 Hz. Independent measurement of the electron density is available from the PIP which also samples at a rate of 1.0 Hz. High time resolution measurements of the ISS frame potential relative to the space plasma environment is obtained from the FPP at a sample rate of 128 Hz. We focus on the FPP measurements for this work because the high sample rate is required to detect the features of the transient floating potential variations that are the topic of this paper.

The FPMU is mounted on an ISS external video camera port that provides power and access to the ISS communications system. FPMU was originally deployed on Camera Port 2 located on the starboard Truss, but the instrument was moved on 21 November 2009 to a new location on Camera Port 6 on the port Truss. Signals from each of the instruments are combined in the FPMU electronics box and converted into a video signal for downlink. The TV Camera Interface Control (TVCIC) provides power to the FPMU and is the interface between FPMU and the ISS communications system. The FPMU video signal is downlinked through the ISS Ku band communications system and transferred to ground stations where the video signal is received and archived. Processing of the raw telemetry data is all accomplished on the ground.

An example of ISS typical ISS charging over an orbit is given in Fig. 3. The FPP measurements of the ISS frame potential shows the oscillatory ($v \times B$) contribution to the potential at the location of the FPMU. A set of negative charging peaks occur at each eclipse exit (marked with red arrows) due to current collection on the PVAs. The charging peaks only persist for a short period following eclipse exit because the SSU's will begin to shunt strings as the batteries are charged and the arrays rotate into plasma wake—reducing the current collection—as the arrays track Sun [22].

Orbital day and night is indicated by the yellow and black bar, respectively, under the potential panel. The middle panel gives the WLP electron density (black) and NLP electron temperature (blue). Features of the ionosphere density present in the data include the daytime equatorial plasma crests and night time plasma depletions at high northern and equatorial

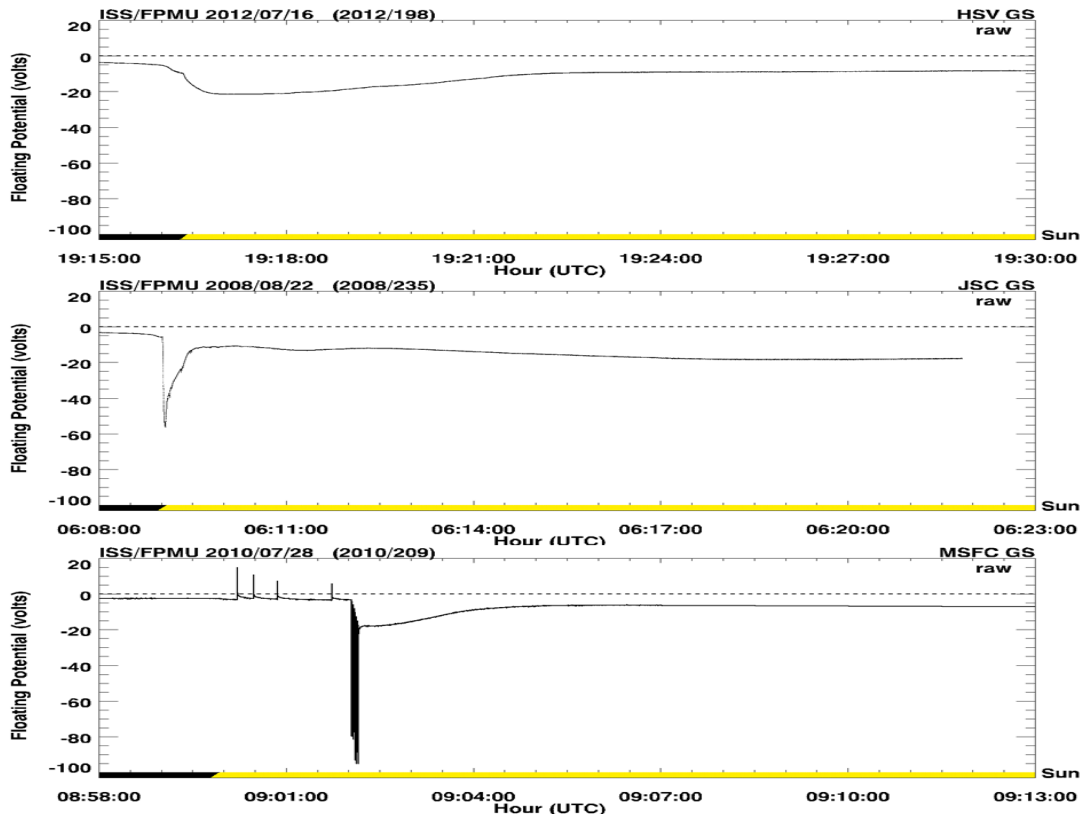


Fig. 4. Examples of negative charging due to current collection on ISS high voltage solar arrays. (top) normal eclipse exit charging, (middle) eclipse exit rapid charging events, and (bottom) rapid charging events in sunlight following array unshunt operations. Positive transients are also present in this plot which are discussed later in the paper (from ref. [11]).

latitudes. ISS latitude and longitude are given in the bottom panel.

IV. ISS NEGATIVE CHARGING

Fig. 4. shows examples of the three basic types of negative charging events which occur following eclipse exit that have been identified in FPMU data. All three types are due to solar array interactions with the plasma environment. The PCU was not operating for these events and the potentials refer to the ISS potential measured by the FPMU floating potential probe at the location of the FPMU instrument.

Potentials due to normal charging (Fig. 4, top panel) are generally in the range of -20V to -30V and the duration of the charging events may last for many minutes to 10's of minutes [21]. Normal charging is the most commonly observed type of ISS eclipse exit charging event. Normal charging is well relatively well understood and comparison of ISS frame potential measurements with ISS charging models are described in [23], [24], and [25].

Rapid charging events at eclipse exit (Fig. 4, middle panel) are characterized by increases in potential over time scales of a seconds followed by a rapid decrease in potential over a few seconds. While many rapid charging events remain within the -20 to -40V range, the example shown here is -65 V. Some of the largest eclipse exit charging events observed on the ISS to date have been rapid charging events with potentials in the -40V to -67V range [26, 27]. Rapid charging events are less common

than normal charging, and appear to be correlated to eclipse exit conditions with low plasma densities (less than $3 \times 10^{10} \text{ m}^{-3}$) [26]. A number of mechanisms have been proposed to explain the physics responsible for the rapid charging events at eclipse exit including current collection on the solar arrays [26] and electric field gradients at the dawn terminator [29]. The solar array current collection mechanism proposed by [28] is favored by the charging community and a number of models have been described by [30, 31, 32] and most recently by [33] and [34].

Finally, a class of rapid charging events (Fig. 4., bottom panel) occur when fully shunted solar arrays are unshunted in full sunlight [26, 27]. Sunlight unshunt rapid charging events are transient events reaching the maximum potential within one FPMU sample period (≤ 7.8 milliseconds) followed by a rapid decrease in potential on times scales of 20 to 150 msec. Sunlight unshunt rapid charging events were first observed on GMT 2010/155 and over the period GMT 2010/205-212 during a set of 36 experiments in which all eight ISS solar arrays were fully shunted for about 3 minutes following eclipse exit. Then each array wing was unshunted at 1 second intervals resulting in a set of eight charging peaks. Additional events have been observed on when array power manipulation activities associated with the ammonia pump repair required shunting the 2B array and unshunting in sunlight [11]. The largest recorded ISS negative charging events fall in this category. Maximum potentials for 288 of the 289 sunlight unshunt rapid charging event charging peaks observed through 2014 are more negative than -45V, 265 events are more negative than -60V, and 16

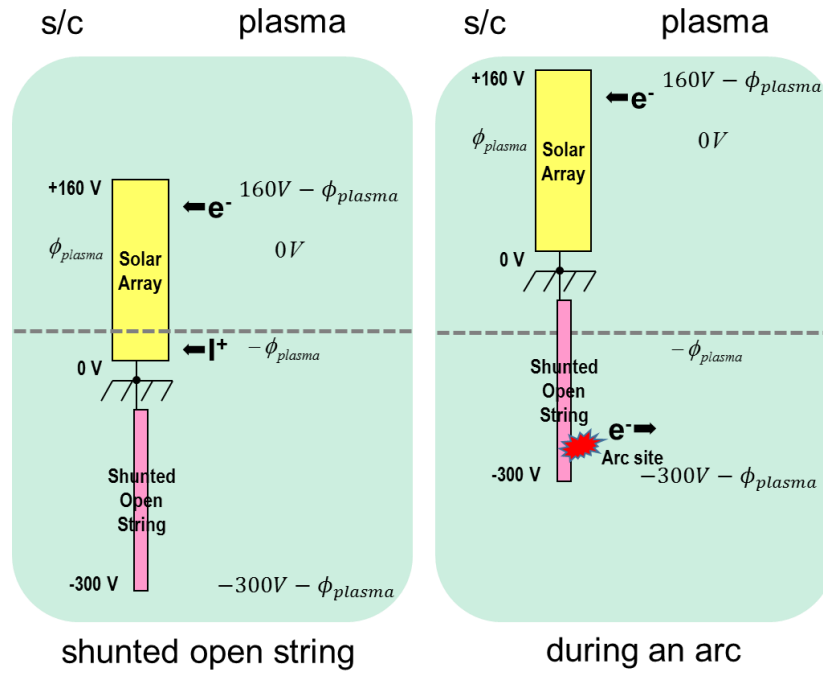


Fig. 5. ISS potentials for a shunted string with an open-circuit fault near the beginning of the string on eclipse exit. The left panel is before and the right panel is during an arc. Note the ISS frame potential, which is the ground, becomes less negative or even positive with respect with respect to the ambient plasma.

events are more negative than -90V. Two charging events on GMT 2010/209 reached -95V and are the largest negative charging events observed to date on the ISS. Sunlight unshunt rapid charging events have been observed in all cases where FPMU data is available following unshunt of a solar array in sunlight.

In addition, to negative charging, a series of four positive charging peaks are present in the bottom panel of Fig. 4 before the arrays are unshunted at about 09:02 UTC. These positive peaks, first reported by [33], are due to a different mechanism than simple solar array current collection and are discussed in the following sections.

V. EVIDENCE OF ISS ARCING ON NEGATIVELY BIASED OPEN STRINGS

In this section, ISS flight data is presented with the unmistakable characteristics of negative potential arcing. This is the first direct evidence of spacecraft charging arcs on the ISS, albeit on the solar arrays, not on an EMU which was the primary concern for arcing that drove the requirement for deploying PCU's on ISS.

Plasma arcing threshold potentials vary widely. Micron thick anodization, like that on the ISS MMOD shield, has been shown in the laboratory to arc at potentials well below -100 V. ISS solar cells have been shown by to arc at potentials between -210 V and -457 V [6]. While negative potentials this large do not appear on ISS solar cells under nominal conditions, there is an open-circuit fault condition, present on some ISS solar array strings, that can cause negative voltages this large. It is known that a number of open-circuit failures exist on the ISS PVAs. Measurements as early as 2002 showed string open-circuit failures on the 2B SAW [10].

A. Open-circuit string faults can cause large negative potentials on solar cells

The solar array string potentials are nominally regulated to 160 V. However, open circuit string voltages when the arrays are cold coming out of eclipse can run as high as 320 V, twice the nominal voltage.

As described in Section II, nominally the low side of solar array strings are tied to ISS chassis ground. Battery charging is controlled by shunting excess array current to ground. Under normal conditions, when both the low and high sides of a string are connected to chassis ground, all the cells in the shunted string are at chassis potential. However, if there is an open circuit somewhere in the string, shunting ties the most positive cell in a string to chassis ground, and all of the connected cells on the high side of the open circuit are at potentials negative with respect to ground. The left panel of Fig. 5 shows this when the open circuit is close to the beginning of the string and most of the cells are connected to the high side. The open circuit cells, although quite negative, collect small ion currents and do not contribute much to the ISS charging with respect to the plasma.

B. Arcs on shunted open-circuit strings can drive the ISS potential positive

As seen in the left panel of Fig. 5, after eclipse exit, the negative potentials on some cells in shunted open-circuit strings are beyond the measured arc threshold. When this occurs, the insulating surfaces near the cells, Kapton® and coverglass, collect ions until their potentials are near that of the local ionosphere. The configuration where the exposed cell edges are negative with respect to the nearby insulators, an inverted potential gradient, leads to arcs whose duration can be extended by potential differences with nearby solar cells [35]. This mechanism of arc initiation and extension has been demonstrated in laboratory tests.

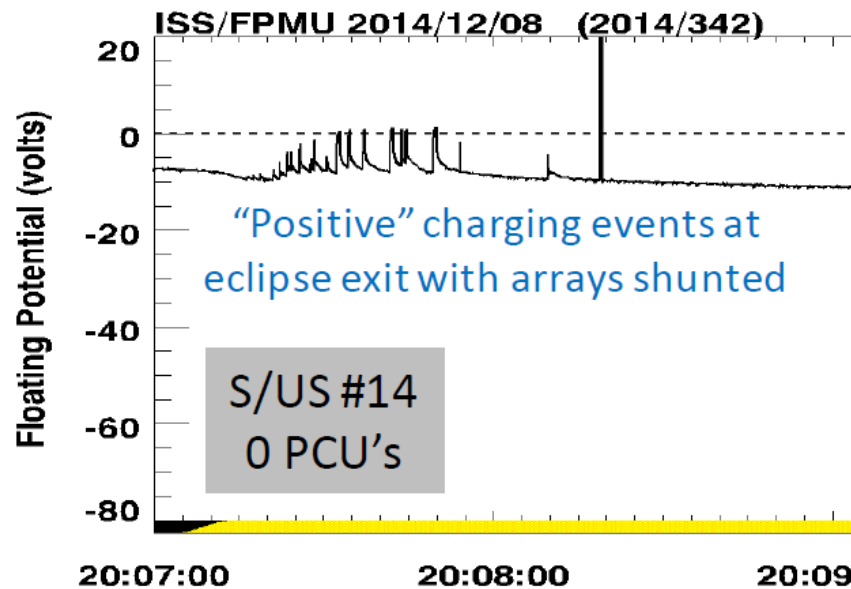


Fig. 6. ISS eclipse exit potential transients measured by the FPMU during Command Shunt/Unshunt experiments on 8 December 2014. The last peak exceeding +20 V is a bad data point. The label “S/US #14” indicates this was the 14th orbit with all arrays shunted as ISS entered sunlight. The unshunt operations were about three minutes into sunlight and are not shown on the plot. “p PCU’s” indicate that the PCU’s were not operating during the experiment.

The plasma generated at an arc site is locally much denser than the surrounding ionospheric plasma. Such arcs can emit ampere level electron currents; i.e., electron emission that is much greater than the ion currents collected by conductors connected to ISS chassis ground. This electron emission causes the chassis potential to jump positively on the most rapid timescale (less than a millisecond) that is determined by sheath charging. As the arc extinguishes, the potentials return to their original configuration on a longer timescale due to the slower charging rate required to recharge the ISS structure.

C. ISS/FPMU data with negative arcing

As discussed above, the conditions for negative arcing on open-circuit strings are most favorable immediately after eclipse exit, when the cells are cold and generate the largest voltage with the high end shunted so that the voltages generated are all negative with respect to ionosphere ground. If the potentials are negative enough to generate an arc, the signature would be a very rapid rise in the ISS potential with respect to the local plasma, followed by a slower decay as the arc extinguishes.

These exact conditions were achieved during ISS Command Shunt/Unshunt experiments performed December 8, 2014. Array shunts for the sunlight unshunt experiments in 2014 were accomplished by powering the Sequential Shunt Unit (SSU) Photovoltaic Control Electronics (PVCE) Off in eclipse and leaving the power off for three minutes into sunlight. Fig. 6 shows the ISS potential with respect to plasma (“floating potential”) as measured by the FPMU/FPP during the first two minutes after eclipse exit.

Right after eclipse exit the floating potential trace shows the characteristic signature of negative potential arcing, rapid rise followed by a slower return. Electron emission from the arc site plasma causes the rapid rise in potential; the slower decay as the arc extinguishing. These events are not unique to this

particular orbit. Similar arc signatures were observed during several eclipse exit tests with shunted arrays.

VI. ADDITIONAL EXAMPLES OF NEGATIVE ARCING

Finally, two additional examples of negative arcing following eclipse exit are shown in Fig. 7 from two orbit segments on 10 February 2013. Standard solar array operations are in progress for both orbits with the SSUs automatically controlling the number of active and shunted strings. No shunt/unshunt experiment is in progress. These examples demonstrate that turning off the arrays by powering off the PVCE during a shunt/unshunt experiment is not required to observe the negative arcing.

The first example of negative arcing is shown in Fig. 7-a for an eclipse exit at about 09:51:20 UTC. FPP measurements of the ISS frame potential are shown in the top panel. The ISS structure potential at the FPMU location is initially about -2 V before ISS encounters sunlight and then increases to a maximum of about -23 V as the vehicle moves into sunlight and the biased solar arrays collect current from the plasma environment.

The middle panel gives a voltage output from the Photovoltaic Control Electronics (PVCE) which is proportional to the number of active strings on each the array with the output color coded for a specific SAW. Voltages of about 27 V indicate all strings are active and the voltage decreases as strings are shunted. The PVCE data is only available at 0.1 Hz from standard ISS telemetry. In this case the arrays are all unshunted as ISS moves into sunlight until about 09:51:39.5 UTC when strings on the 3B SAW are shunted and a large negative arcing event is observed. The second negative arcing event occurs at about 09:51:47.4 UTC, just before the next available PVCE shunt state data indicating the 3B strings are still shunted and strings on the 2A, 4A, and 4B SAW were

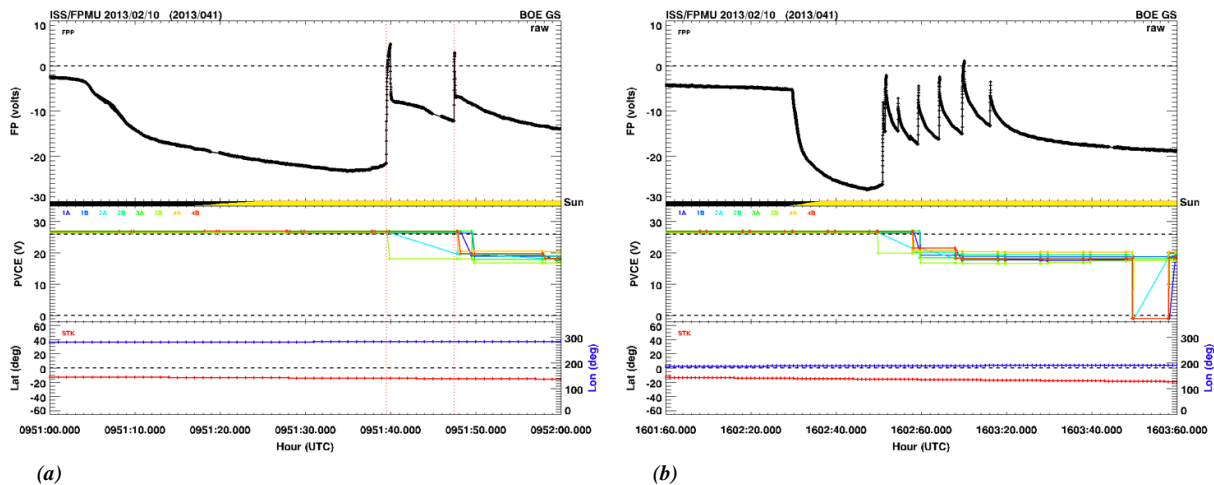


Fig. 7. Examples of negative arcing on 10 February 2013 following eclipse exit at (a) 09:51:20 UTC and (b) 16:02:30 UTC. Both of these examples are for normal ISS solar array operations with no shunt/unshunt experiment in progress. FPP potentials (top panel) show arcing events in both data sets. PVCE voltages (middle panel) are proportional to the number of shunted strings on each SAW with the color coding indicating which SAW is shunted. A “rainbow” color scale from blue through red are used for the 1A, 1B, 2A, 2B, 3A, 3B, 4A, and 4B SAWs. ISS latitude (red) and longitude (blue) are given in the bottom panel.

shunted some time during the 10 second period between the PVCE samples.

The second example of negative arcing from an eclipse exit later on the same day at about 16:02:30 UTC is shown in Fig. 7-b where eight arcing events are observed once shunt operations begin on the arrays. ISS frame potential decreases from -4 V before the vehicle enters sunlight -27 V as the biased arrays collect current in sunlight. The first negative arcing event decreases the frame potential to about -8 V followed immediately by a second event that decreases the frame potential to about -2 V. Six additional negative arcing events follow that remove varying amounts of charge from ISS. Note that the recharge time to collect additional electron current between the events exhibit the same time constant for each event.

The initial ISS solar array charging in both cases shown in Fig. 7 appear to start before sunlight is present on the vehicle. This is an artifact of the method we are using to compute insolation at the location of ISS. The ISS ephemeris and solar illumination at the ISS location is computed using the Satellite Tool Kit® (STK) software. The STK model for solar illumination does not account for effects of the Earth’s atmosphere and gives 0% illumination at first contact of the solar disk with the Earth’s horizon and 100% illumination at final contact. Orbital sunrise is actually earlier than first contact due to scattering of sunlight through the Earth’s atmosphere. Solar arrays are sensitive to light on the red end of the spectrum which is preferentially scattered through the atmosphere resulting in biased arrays at times before the STK algorithm predicts light at the ISS location [c.f., 36].

VII. CONCLUSION

We reported a new class of transient ISS frame potential variations consistent with negative arcing on open-circuit solar array strings using data from the ISS FPMU FPP instrument. The transients are characterized by a rapid decrease in the negative frame potential to values less negative, or even positive, than the equilibrium potential followed by a gradual

return to equilibrium conditions. The events are always observed in sunlight when the PVAs are biased and occur during periods when some or all of the PVA strings are shunted consistent the proposed model that the arcs occur on open-circuit, shunted strings. Open circuit strings can exhibit voltages exceeding -300 V when the strings are shunted. Under these conditions the local potential on the damaged string can easily exceed arcing thresholds at the low end of the -210 V to -457 V range for ISS PVAs. Because arcing to space on the array will remove some fraction of the net negative charge on the ISS, transient variations in the frame potential are expected during the electrostatic discharge events.

ACKNOWLEDGMENT

Financial support for this work was provided by NASA’s Engineering and Safety Center through technical assessment TI-16-01108.

REFERENCES

- [1] A.C. Tribble, *The Space Environment – Implications for Spacecraft Design*, Princeton University Press, ISBN 978-0691102993, 1995.
- [2] NASA-HDBK-4006A, *Low Earth Orbit Spacecraft Charging Design Handbook*, 2018.
- [3] M.R. Patel, *Spacecraft Power Systems*, CRC Press, Boca Raton, FL, 2005., pp 422 – 423.
- [4] T. A. Schneider, T. A., et al., “Minimum Arc Threshold Voltage Experiments on Extravehicular Mobility Unit Samples,” AIAA-2002-1040, January 2002.
- [5] T. P. Black, T.A. Schneider, J. A. Vaughn, B. R. Tiepel, L. Kramer, and P. L. Leung, “Plasma-Induced Dielectric Breakdown of Anodized Aluminum Surfaces,” AIAA-2006-871, January, 2006.
- [6] H. K. Nahra, M. C. Felder, B. L. Sater, and J. V. Staskus, “The Space Station Photovoltaic Panels Plasma Interaction test Program: Test Plan and Results,” AIAA-90-0722, January, 1990.
- [7] J.I. Minow, “Development and Implementation of an Empirical Ionosphere Variability Model,” *Adv. Space Res.*, 33, 887 – 892, 2004.
- [8] *International Space Station Familiarization*, Johnson Space Center, TD9702A, Houston, TX, 1998.
- [9] E. Gietl, E. W. Gholdston, B. A. Manners, and R. A. Delventhal, “The Electric Power System of the International Space Station – A Platform for Power Technology Development,” NASA TM-2000-210209, June 2000.

- [10] T.W. Kerslake and E. D. Gustafson, "On-Orbit Performance Degradation of the International Space Station P6 Photovoltaic Arrays," NASA TM-2003-212513 (AIAA-2003-5999), July, 2003.
- [11] A. Hernandez-Pellerano, C. J. Iannello, H. B. Garrett, A. T. Ging, I. Katz, R. L. Keith, J.I. Minow, E. Willis, T.A. Schneider, A. C. Whittlesey, and E. J. Wollack, and K. H. Wright, "International Space Station (ISS) Plasma Contactor Unit (PCU) Utilization Plan Assessment Update," NASA TM-2014-218512 (NESC-RP-13-00869), August, 2014.
- [12] M.R. Carruth, Jr., T. Schneider, M. McCollum, M. Finckenor, R. Suggs, D. Ferguson, I. Katz, R. Mikatariyan, J. Alred, and C. Pankop, "ISS and Space Environment Interactions without Operating Plasma Contactor," AIAA-2001-401, *Aerospace Sciences Meeting and Exhibit, 39th*, Reno, Nevada, January 9-11, 2001.
- [13] E. M. Willis, J. I. Minow, M. Z. A. Pour, K.-I. Nishikawa, and C. Swenson, "Transient Floating Potential Variations Attributed to High-Voltage Solar Array Operations," *J. Spacecraft Rockets*, 54, 1127 – 1138, 2017.
- [14] Koontz, S.L., L. Kramer, R.R. Mikatariyan, and C.E. Soares, Section 8.6: Spacecraft charging hazards, in *Safety Design for Space Operations*, edited by F.A. Allahdadi, I. Rongier, P. Wilde, and T. Sgobba, Elsevier Ltd., 2013.
- [15] M. J. Patterson et al., "Space Station Cathode Design, Performance, and Operating Specifications," presented at the 25th International Electric Propulsion Conference Proceedings, IEPC-97-170, August 24--28, 1997.
- [16] S. D. Kovalski, M. J. Patterson, G.C. Soulas, and T.R. Sarver-Verhey, "A Review of Testing of Hollow Cathodes for the International Space Station Plasma Contactor," NASA/TM-2001-211291, presented at the 27th International Electric Propulsion Conference Proceedings, IEPC-01-271, October 14--19, 2001.
- [17] C. Swenson, D. Thompson, and C. Fish. The Floating Potential Measurement Unit, AIAA-2003-1081, *41st Aerospace Sciences Meeting and Exhibit*, Reno, Nevada, 2003.
- [18] C. Swenson, D. Thompson, and C. Fish. The ISS Floating Potential Measurement Unit, *9th Spacecraft Charging Technology Conference*, JAXA-SP-0F-001E, Japan Aerospace Exploration Agency, April 2005.
- [19] A. Barjatya, A., Langmuir Probe Measurements in the Ionosphere, *PhD Dissertation, University of Utah*, Logan, Utah, 2007.
- [20] A. Barjatya, C. M. Swenson, D. C. Thompson, and K. H. Wright, Jr., Invited article: Data analysis of the Floating Potential Measurement Unit aboard the International Space Station, *Rev. Sci. Instruments*, 80, 041301, 2009.
- [21] K. H. Wright, Jr., C. M. Swenson, D. C. Thompson, A. Barjatya, S. L. Koontz, T. A. Schneider, J. A. Vaughn, J. I. Minow, P. D. Craven, and V. N. Coffey, "Charging of the International Space Station as Observed by the Floating Potential Measurement Unit: Initial Results," *IEEE Transactions on Plasma Science*, Vol. 36, No. 5, 2008, pp. 2280–2293.
- [22] J. Alred, R. Mikatariyan, and S. Koontz, "Impact of Solar Array Position on ISS Vehicle Charging," AIAA-2006-868, January, 2006.
- [23] M. J. Mandell, V.A. Davis, B. Gardner, and G. Jongeward "Electron Collection by International Space Station Solar Arrays," presented at the 8th Spacecraft Charging Technology Conference, Huntsville, AL, 20-24 October 2003.
- [24] R. Mikatariyan, H. Barsamian, J. Kern, S. Koontz, and J.F. Roussel, "Plasma Charging of the International Space Station," presented at the 53rd International Astronautical Congress, The World Space Congress – 2002, 10 - 19 Oct 2002, Houston, Texas, IAC-02-T.2.05.
- [25] B. Reddell, J. Alred, L. Kramer, R. Mikatariyan, J. Minow, and S. Koontz, "Analysis of ISS Plasma Interaction," AIAA-2006-865, January, 2006.
- [26] P. D. Craven, K. H. Wright, Jr., J. I. Minow, V. N. Coffey, T. A. Schneider, J. A. Vaughn, D. C. Ferguson, and L. N. Parker, "Survey of International Space Station Charging Events," AIAA-2009-0119, *47th AIAA Aerospace Sciences Meeting and Exhibit*, Orlando, FL, Jan. 5-8, 2009.
- [27] J. I. Minow, K. H. Wright, Jr., M. O. Chandler, V. N. Coffey, P. D. Craven, T. A. Schneider, L. N. Parker, D. C. Ferguson, S. L. Koontz, and J. W. Alred, "Summary of 2006 to 2010 FPMU Measurements of International Space Station Frame Potential Variations," 11th Spacecraft Charging Technology Conference, Albuquerque, New Mexico, 20 - 24 September 2010.
- [28] D. C., Ferguson, Craven, P. D., Minow, J., and Wright, K., "A Theory for Rapid Charging Events on the International Space Station," AIAA Atmospheric and Space Environments Conference, AIAA Paper 2009 3523, 2009.
- [29] S. J. Koontz, J. Alred, L. Kramer, D. Hartman, R. Mikatariyan, and K. Smith, "Measuring Ionospheric Electric Field Gradients with the International Space Station Floating Potential Probe," Biennial Research and Technology Development Report, Johnson Space Center, 53, 2009.
- [30] D. Hui, "A Model for Rapid Charging Events on the International Space Station," M.S. Thesis, Utah State Univ., Logan, UT, 2011.
- [31] J. Huang, Z. Yi, H. Zhao, L. Meng, and Y.Liu, "Model for Rapid-Charging Events for the International Space Station," *J. Spacecraft and Rockets*, vol. 51, No. 1, pp 11 – 15, 2014a.
- [32] J. Huang, Z. Yi, H. Zhao, L. Meng, and Y.Liu, "Mechanism for Rapid Charging Events on International Space Station," *J. Spacecraft and Rockets*, vol. 51, No. 3, pp 917 – 921, 2014b.
- [33] E. M. Willis, J. I. Minow, M. Z. A. Pour, K.-I. Nishikawa, and C. Swenson, "Transient Floating Potential Variations Attributed to High-Voltage Solar Array Operations," *J. Spacecraft Rockets*, 54, 1127 – 1138, 2017.
- [34] E. Willis and M. Pour, "A New Model for Plasma Interactions with High Voltage Solar Arrays on the International Space Station," *IEEE Trans. on Plasma Sci.*, Vol. PP, Issue 99, pp 1-9, 2018. DOI: 10.1109/TPS.2018.2808099.
- [35] I. Katz, V. A. Davis, and D. B.Snyder, "Mechanism for Spacecraft Charging Initiated Destruction of Solar Arrays in GEO," 36th AIAA Aerospace Sciences Meeting and Exhibit, AIAA 1998-1002., 1998.
- [36] D. C. Ferguson, P. D. Craven, and J. I. Minow, "The Effects of Eclipse-Exit Weather and Magnetic Latitude on ISS Rapid-Charging Events," AIAA-2010-332, January, 2010.